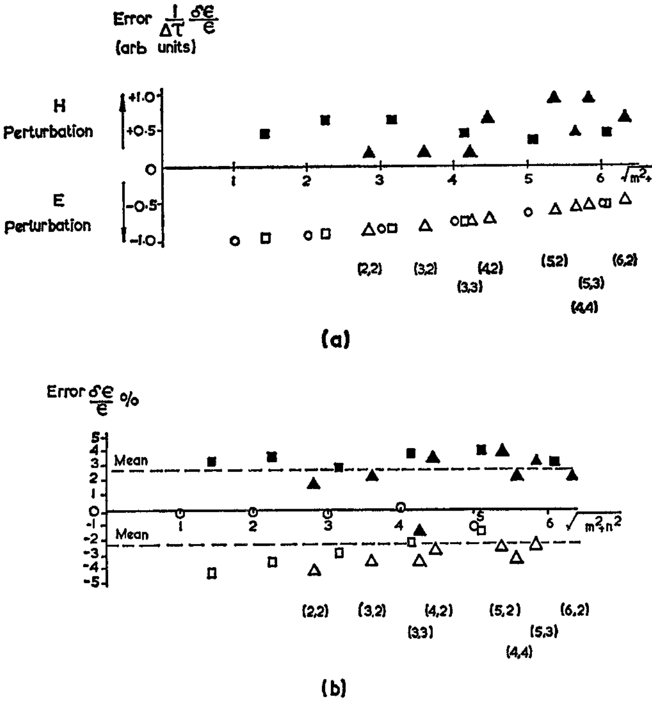

Fig. 4. Mode errors in ϵ_{xx}. (a) Theoretical. (b) Experimental (averaged over 15 samples).

theoretical error and seeing if, as a consequence, there results a discrepancy between theory and experiment that can be accounted for qualitatively by the omitted (magnetic) term (see the discussion on Fig. 4).

For electric sidewalls, $\boldsymbol{n}\cdot\boldsymbol{H}=0$ at all interior metal surfaces. The cutting of an aperture replaces an element δS of this surface by $\delta S'$, at which $\boldsymbol{n}\times\boldsymbol{H}=0$, and across which the magnetic field must pass normally [Fig. 3(b)]. Insofar as the overlaid stripline constitutes an unchanged boundary condition for $\boldsymbol{E}$, there is a comparatively small change in the electric field, so that the second term in (2) dominates the frequency shift for this coupling method. The effect upon ϵ_{xx} can be calculated from the following equation, derived from (1) and (2):

$$\left.\frac{\delta\epsilon}{\epsilon_{xx}}\right|_{m,n} \alpha \int_{\Delta\tau} (H^2 - E^2)\, dv. \quad (3)$$

If the variation in phase over the coupling regions is neglected, and account is taken of only the electric contribution for the $(n, 0)$ frequencies, the error as a function of mode index $\sqrt{m^2+n^2}$ comes to the values set out in Fig. 4(a). The corresponding experimental points, expressed as averages over the 15 samples, are given in Fig. 4(b). Except for the $(n, 0)$ modes, the relative placement of the error points is broadly correct. The discrepancy for the zero-order resonances clearly shows that the magnetic energy in the cavity is increased by the field penetrating from the lines into the edges normally having $\boldsymbol{n}\cdot\boldsymbol{H}=0$, as was discussed in the application of (2) to the magnetic-sidewall cavity, and has the desirable effect of reducing the measurement error, in our experiments, to within 0.5 percent of the mean defined in Fig. 2. Hence, these modes alone may be used without correction for an accurate characterization of the dielectric over the band.

In general, the observed effect of decreased coupling is to reduce the error for magnetic sidewalls, but to increase it, if anything, for electric sidewalls (see Fig. 2). With corner excitation, the lower bound on the coupling is set by the sensitivity of the apparatus, and in the above experiments gave a mean error in ϵ_{xx} of -2.2 percent with all modes discernable [lower mean in Fig. 4(b)]. The result for aperture excitation can be understood if the feeding stripline is considered as a current boundary condition which limits the leakage of magnetic field $\boldsymbol{H}$. The mean error in this case was $+2.7$ percent [upper mean in Fig. 4(b)]. Thus for any given sample, the permittivity averaged over all modes (which neglects possible dispersion effects) should be within order 0.5 percent of the true value (Fig. 2 gives an example).

TABLE I

Material	Relative Permittivity ϵ_{xx}
Al_2O_3(96%)	8.76
Crystalline Al_2O_3 ("sapphire")	9.34 (base plane) 11.49 (c-axis)
SiO_2 (Fused quartz)	3.85

In conclusion, we have shown that, depending upon the equipment sensitivity, errors of 2–3 percent in the dielectric constant, as deduced from cavity-resonance measurements, can arise from the system of coupling. Two complementary methods of excitation have been described which, because they give rise to errors of opposite sense, improve the accuracy of the averaged dielectric constant to order 0.5 percent. For quick answers requiring no correction, the zero-order resonances of an uncoated sidewall cavity can be used to accurately measure the dielectric constant over the band. Our results for the common materials in the frequency range 2–12 GHz as determined by these methods are shown in Table I.

Acknowledgment

The authors wish to thank J. Tame and Mrs. C. Garrett for their assistance in metallizing the samples, and Dr. H. F. Lenzing of Bell Telephone Laboratories for a reprint of [2].

References

[1] L. S. Napoli and J. J. Hughes, "A simple technique for the accurate determination of the microwave dielectric constant for microwave integrated circuit substrates," *IEEE Trans. Microwave Theory Tech.* (Corresp.), vol. MTT-19, pp. 664–665, July 1971.
[2] H. F. Lenzing, "Measurement of dielectric constant and ceramic substrates at microwave frequencies," *Amer. Ceram. Soc. Bull.*, vol. 51, p. 361, 1972.
[3] R. E. Collin, *Field Theory of Guided Waves.* New York: McGraw-Hill, 1960.
[4] J. C. Slater, *Microwave Electronics.* Princeton, N. J.: Van Nostrand, 1950.
[5] E. L. Ginzton, *Microwave Measurements.* New York: McGraw-Hill, 1957.
[6] J. Q. Howell, "A quick accurate method to measure the dielectric constant of microwave integrated-circuit substrates," *IEEE Trans. Microwave Theory Tech.* (Short Paper), vol. MTT-21, pp. 142–143, Mar. 1973.

Equivalent Representation of an Abrupt Impedance Step in Microstrip Line

R. HORTON

***Abstract*—The equivalent electrical lengths of uniform microstrip line associated with an abrupt impedance step are first evaluated, under static assumptions. The importance of these results in establishing a reference plane for the step, and in the application of calculations of capacitance associated with the step, is then demonstrated.**

Furthermore, some interesting dualities are discerned from the results.

Introduction

The evaluation of equivalent circuits associated with common microstrip discontinuities has recently been a subject of intense interest in the microwave field, and the analysis of discontinuities causing predominantly capacitative effects, such as open-circuits or gaps, has received much attention from such workers as Farrar and Adams [1], Silvester and Benedek [2], Jain *et al.* [3], and Maeda [4].

However, discontinuities with associated inductive and capacitative effects, such as bends, impedance steps, and T junctions, have received less attention to date, due to the more involved problem. Nevertheless, attempts have been made by Wolff *et al.* [5], Horton

Manuscript received December 14, 1972; revised April 2, 1973.
The author is with the Advanced Techniques Branch, Australian Post Office, Research Laboratories, Melbourne, Vic., Australia.

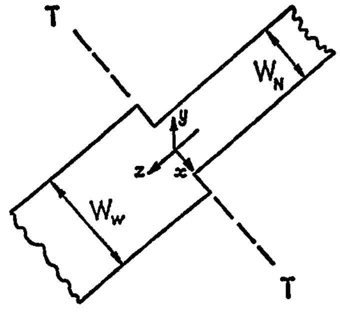

Fig. 1. Upper-strip configuration of an impedance step.

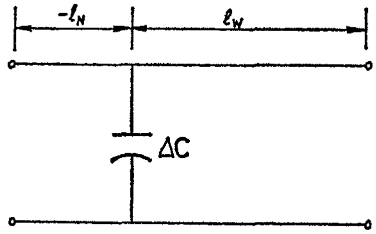

Fig. 2. Equivalent circuit of the impedance step.

[6], and Farrar and Adams [1]. The latter ignores the inductive effects of an impedance step with caution.

In this short paper, an approach to the calculation of the equivalent lengths of uniform microstrip line associated with an abrupt impedance step is outlined, basing the calculations on the static current paths occurring with such a structure. Because of these assumptions, the limitations of quasi-TEM propagation are therefore imposed and, for the geometries investigated, an upper limit of about 12 GHz is expected for good experimental agreement.

Having established these equivalent lengths of line ascribable to the step, a reference plane can then be delineated, and the necessity of this total information in the calculation of capacitance, due to the step, is demonstrated by its application to the theory of Farrar and Adams [1], yielding results corrected for the effect of inductance.

It is worthwhile to mention that some meaningful dualities between the magneto- and electrostatic approaches can be deduced from the outcome of the calculations, and it was concluded that an exclusively electrostatic approach could provide information on the inductive and capacitative components, provided the extensions given later in this short paper were applied.

Equivalent Lengths of Microstrip Line Associated with an Abrupt Impedance Step

The step in impedance, resulting from an abrupt change in width of the upper conductor of the microstrip configuration, is shown in Fig. 1, where W_w and W_N represent the widths of the wide and narrow lengths of line comprising such a step.

The inductive and capacitative effects of the field distortions caused by the discontinuity have been calculated with the aim of achieving the parameters of the equivalent circuit shown in Fig. 2, where l_w and $-l_N$ represent lengths of uniform line of widths W_w and W_N, respectively, and ΔC represents the additional capacitance associated with the step.

To estimate the values of l_w and $-l_N$, the static current path was investigated in the region of the discontinuity; this was accomplished under the initial assumption of the step comprising two semi-infinite lengths of uniform microstrip line of widths W_w and W_N jointed at plane T–T of Fig. 1. Each of these lines was assumed to be carrying currents $J_{Z_w}(x)$ and $J_{Z_N}(x)$, respectively, undisturbed by the juncture, where $J_{Z_w}(x)$ is the current profile supported by an infinitely long microstrip line of width W_w, and $J_{Z_N}(x)$ is that for width W_N. $J_{Z_w}(x)$ and $J_{Z_N}(x)$ can be estimated through the integral equation, as in [6]:

$$\phi(x) = \int_x G_M J_Z(x)\, dx \tag{1}$$

where this equation is numerically inverted to provide longitudinal components $J_{Z_{N,w}}(j)$ of a subsectioned cross section of infinite line. G_M represents the two-dimensional Green's function of the problem, while $\phi(x)$ represents the total normal flux passing through a y–x plane contained by the double-sided strip version of the infinitely long line. In numerical form, (1) becomes

$$[\phi_i] = [G_{Mi,j}][J_j]. \tag{2}$$

Assuming continuity of the total normal flux contained between strips permits an arbitrary equal value to be assigned to all elements ϕ_i, thereby facilitating the inversion of (2).

Imposing the condition of continuity of current at the junction T–T gives the normalization

$$\sum_{\substack{\text{cross}\\\text{section}}} J_{j_N} = \sum_{\substack{\text{cross}\\\text{section}}} J_{j_w}. \tag{3}$$

Going on to a three-dimensional representation of an infinitely long line, and with the continuing assumption of an absence of dielectric, the instantaneous charge profile can be generated from the current profile $J_Z(x)$ and used to provide a profile of instantaneous potential $V(x, z)$ existing on the upper infinitely long strip via an integral equation of the form

$$V(x, z) = \int_{x,z} G_{E_0} q_z(x)\, dx dz. \tag{4}$$

Equation (4) is realized numerically by the square subsectioning of the infinite uniform line. G_{E_0} represents the Green's function of this relationship and $q_z(x)$ the assumed point charges located at the center of each square subsection. In numerical form, (4) becomes

$$V[i, j] = [G_{E_{0i,j}}][q_j]. \tag{5}$$

The outcome of (6) is, of course, to provide a contour of instantaneous electrostatic potential, which is constant and independent of longitudinal position for the infinite uniform line to any prescribed numerical satisfaction.

Reverting to the original model of two semi-infinite lines butted together and carrying longitudinal current profiles $J_{Z_N}(x)$ and $J_{Z_w}(x)$, once more with an absence of dielectric, the three-dimensional relationship of (5) may be applied to a square-subsectioned region of the discontinuity at plane T–T to give a profile of instantaneous conductor potential in this region. This conductor potential varies continuously throughout the region and can be compared with the constant potential profiles obtained with infinitely long uniform lines of widths W_w and W_N supporting the same current profiles $J_{Z_w}(x)$ and $J_{Z_N}(x)$. The resulting differences in potential along the z direction of Fig. 1 can then be numerically assessed in incremental steps, and as the potentials are proportional to the square root of inductance at any point z, the variation of inductance in the region of the discontinuity can be determined and interpreted as a continuous change of phase velocity. This continuous change can in turn be summated to produce equivalent lengths of uniform lines $-l_N$ and l_w existing on either side of plane T–T.

Going on to the case where dielectric is present, this is expected to have negligible effect on the longitudinal current profiles assumed, below the limit of 12 GHz. The magnitude of the instantaneous charge profile is, however, scaled up by the inverse ratio of phase velocity for both cases of dielectric present and absent. Nevertheless, the lowering of phase velocity in the presence of dielectric compensates this effect and leads to the conclusion that the deviation of inductance encountered, compared with that of a TEM wave supported by a uniform infinitely long strip, is the same whether dielectric is present or not, and the interpretation of absolute lengths l_w and $-l_N$ holds in both cases.

Calculation of Capacitance Associated with the Impedance Step

As has been stated, the theoretical approach of Farrar and Adams, in which the excess capacitance associated with a finite region of conductor (including the impedance step) was investigated, gave results which neglected any inductive effects and which will be shown to be accurate over a limited aspect ratio only.

Summarizing their approach, the additional capacitance ΔC was estimated using the expression

$$\Delta C = \lim_{L\to\infty} [C_t(L) - C_{oc}(1) - C_{oc}(2) - C_{01}L - C_{02}L] \tag{6}$$

where C_{oc} (1) and C_{oc} (2) are the open-circuit lumped capacitances

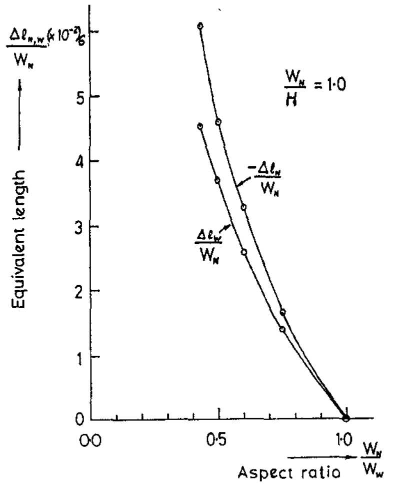

Fig. 3. Equivalent lengths of uniform lines ascribable to the impedance step.

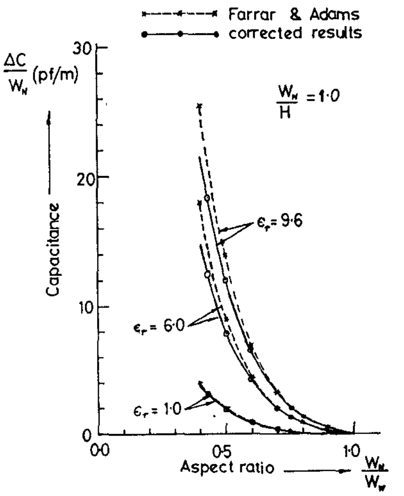

Fig. 4. Additional capacitance associated with the impedance step.

of lines of widths W_w and W_N, respectively, and C_{01} and C_{02} are the capacitances per unit length of the infinite (two-dimensional) lines of widths W_w and W_N. The two conjoining lines of lengths L create the region investigated, which has a total capacitance $C_t(L)$.

In light of lengths l_w and $-l_N$ calculated in the previous section, a corrected form of (6), accounting for the effects of inductance, is now

$$\Delta C = \lim_{L\to\infty} \left[C_t(L) - C_{oc}(1) - C_{oc}(2) - C_0(L + l_N) - C_{02}(L - l_N)\right]. \quad (7)$$

Results

The equivalent lengths l_w and $-l_N$, in normalized form, associated with a range of aspect ratios W_N/W_w, are shown in Fig. 3 for a constant ratio of $W_N/H = 1.0$, H being the strip-ground plane spacing, which was taken to be 0.025 in. These results supply the necessary information to establish a reference plane for the junction.

The results of Fig. 3 were then applied to (7), giving the corrections required of the capacitance values attained by Farrar and Adams, and these are given in Fig. 4, where their results can be seen to concur well for only a limited aspect ratio.

Of particular interest is the outcome of the comparison of computed results, in the case $\epsilon_r = 1.0$, for both (6) and (7), which indicates (within the numerical error limits) the dualities involved. This case of an absence of dielectric can be accounted for by the effect of series inductance or shunt susceptance on uniform transmission-line behavior, and one would suspect that the definition of an electrical reference plane for the junction would correspondingly produce the same answer. If, in the electrostatic case, the excess and deficiency of charge or capacitance on either side of reference plane T–T had been furnished, then for $\epsilon_r = 1.0$, lengths l_w and $-l_N$ could be discerned, and thus not only provide the reference plane required, but also make available self-correcting measures for the final calculation of capacitance, therefore producing a more representative equivalent.

In conclusion, extended information on the parameters associated with an impedance step have been presented, accounting for both inductance and capacitance, using static assumptions. The interpretation of dualities has enabled comparisons to be made with other theoretical work; these have proven to be extremely good. Furthermore, inferences may be drawn as to the complete adequacy of an exclusively electrostatic approach in the present application.

Acknowledgment

The author would like to thank the Australian Post Office for their permission to publish these results.

References

[1] A. Farrar and A. T. Adams, "Matrix methods for microstrip three-dimensional problems," *IEEE Trans. Microwave Theory Tech.*, vol. MTT-20, pp. 497–504, Aug. 1972.
[2] P. Silvester and P. Benedek, "Equivalent capacitances of microstrip open circuits," *IEEE Trans. Microwave Theory Tech.*, vol. MTT-20, pp. 511–516, Aug. 1972.
[3] O. P. Jain, V. Makios, and W. J. Chudobiak, "Open-end and edge effect in microstrip transmission lines," *IEEE Trans. Microwave Theory Tech.*, vol. MTT-20, pp. 626–628, Sept. 1972.
[4] M. Maeda, "An analysis of gap in microstrip transmission lines," *IEEE Trans. Microwave Theory Tech.*, vol. MTT-20, pp. 390–396, June 1972.
[5] I. Wolff, G. Kompa, and R. Mehran, "Calculation method for microstrip discontinuities and T-junctions," *Electron. Lett.*, vol. 8, pp. 177–179, Apr. 6, 1972.
[6] R. Horton, "The electrical characterization of a right-angled bend in microstrip line," *IEEE Trans. Microwave Theory Tech.* (Short Paper), vol. MTT-21, pp. 427–429, June 1973.

Discontinuity Capacitance of a Coaxial Line Terminated in a Circular Waveguide: Part II—Lower Bound Solution

EDWARD W. RISLEY, JR.

***Abstract*—This calculation provides a lower bound (complementing the upper bound solution given earlier) to the discontinuity capacitance of a coaxial line terminated in a circular waveguide. A 50-Ω 0.9525-cm (3/4-in) open-circuited coaxial termination with a solid center conductor was fabricated with center- and outer-conductor diameters of 0.82723 ± 0.00005 and 1.90487 ± 0.00005 cm (1 cm = 0.393703 in), respectively. The measured value of capacitance of this termination at 1000 Hz was 216.4 ± 1.0 fF, as compared with the calculated lower bound of 215.0 fF. (The upper bound for this case was 217.7 fF.)**

I. Introduction

The standard of reflection for a coaxial line is the quarter-wave short-circuit termination. There are, however, shortcomings to this standard: the fabrication cost is high and each termination is usable at only one frequency. However, an open-circuited coaxial line with an extended outer conductor and a solid inner conductor could be used advantageously as a standard termination, because fabrication can be made using commercially available components and because the device is broad banded and losses are minimal. In addition to the high-frequency application, the device can also be used at low frequencies as a standard of capacitance.

In this short paper, the input impedance Z is formulated in terms of the magnetic field which leads to a lower bound solution for the discontinuity capacitance. Z is expressed as a stationary functional with a definite integral operator, and can therefore be shown to be bounded on the set of admissible trial functions [1].

This result complements the upper bound solution given in an earlier paper [2].

II. Integral Equation for Input Impedance

To derive the stationary form for the input impedance, assume an incident T wave propagating in the direction of increasing z (Fig. 1). Symmetry dictates that only E modes, independent of ϕ,

Manuscript received January 17, 1973; revised March 19, 1973.
The author is with the Circuit Standards Section, Electromagnetics Division, Institute for Basic Standards, U. S. Department of Commerce, National Bureau of Standards, Boulder, Colo. 80302.